Urea and Guanidinium Chloride Denature Protein L in Different Ways in Molecular Dynamics Simulations

C. Camilloni,* A. Guerini Rocco,[†] I. Eberini,[†] E. Gianazza,[†] R. A. Broglia,*[‡] and G. Tiana*

*Department of Physics, University of Milano and INFN, I-20133 Milan, Italy; [†]Gruppo di Studio per la Proteomica e la Struttura delle Proteine, Dipartimento di Scienze Farmacologiche, Università degli Studi di Milano, I-20133 Milan, Italy; and [‡]The Niels Bohr Institute, University of Copenhagen, DK-2100 Copenhagen, Denmark

ABSTRACT   In performing protein-denaturation experiments, it is common to employ different kinds of denaturants interchangeably. We make use of molecular dynamics simulations of Protein L in water, in urea, and in guanidinium chloride (GdmCl) to ascertain if there are any structural differences in the associated unfolding processes. The simulation of proteins in solutions of GdmCl is complicated by the large number of charges involved, making it difficult to set up a realistic force field. Furthermore, at high concentrations of this denaturant, the motion of the solvent slows considerably. The simulations show that the unfolding mechanism depends on the denaturing agent: in urea the β-sheet is destabilized first, whereas in GdmCl, it is the α-helix. Moreover, whereas urea interacts with the protein accumulating in the first solvation shell, GdmCl displays a longer-range electrostatic effect that does not perturb the structure of the solvent close to the protein.

INTRODUCTION

Denaturation has long been used as a tool to probe the folding properties of proteins (1–3), and, in recent years, the denatured state has gained increasing attention because of its importance for understanding the folding process (4). The denaturing agents most largely employed in folding/unfolding experiments are urea and guanidinium chloride (GdmCl).

A central problem concerning this kind of experiment is whether one can define a denaturation process simply, independent of the denaturing agent. Privalov and colleagues (5,6) gave a clear answer to this issue, concluding that the thermodynamic properties associated with protein unfolding do not depend on the denaturing agent, whereas the structural properties do. In other words, the net denaturation enthalpies and entropies are intrinsic properties of proteins, whereas the loss of secondary structures, of compactness, of buried surface, and so on depend on the specific way in which these proteins are denatured.

Because protein folding/unfolding is usually monitored through the analysis of structural features (secondary structure by circular dichroism, burial of tryptophans by fluorescence, etc.) and not through direct calorimetric measurements, it is important to evaluate the effects of the specific denaturing agent.

The situation is further complicated by the fact that the molecular basis for denaturation by urea and GdmCl is still unclear. Two models have been proposed, one based on a direct, favorable interaction between the denaturant and the protein (7,8) and the other based on a modification of the hydrogen-bond structure of water and a consequent weakening of hydrophobic interactions (9). Although both models can explain denaturation curves (10), midinfrared spectroscopy experiments have shown (11) that the dynamics of hydrogen bonds is weakly affected by urea, suggesting that the hydrophobic interaction is not hindered. Moreover, studies of the end-to-end diffusion of unstructured peptides agree (12) with a model in which urea and GdmCl interact homogeneously with all the amino acids with binding constants 0.26 M^{-1} and 0.62 M^{-1}, respectively.

To gain insight into the denaturing effects of urea and GdmCl, we studied the unfolding of the IgG binding domain of Protein L, a 62-residue protein built of a β-hairpin, an α-helix, and another β-hairpin, and that folds following a two-state model (13). Fluorescence experiments in 2 M GdmCl suggest that the first β-hairpin of Protein L is partially structured in the denatured state (14). A ϕ-value analysis based on folding/unfolding obtained again with GdmCl indicates that the helix is largely disrupted in the transition state (15).

In the following section, we introduce a model for GdmCl and describe full-atom, explicit-solvent simulations, performed in both urea and GdmCl, starting from the native conformations and following the disruption of native structural elements. The goal is to understand at a molecular level the destabilization mechanism associated with common chemical denaturants. The elucidation of the differences among urea, guanidinium, and thermal denaturation will be useful both to experimentalists, to interpret correctly the results of experiments, and to theoreticians, to obtain a further insight into the stabilization mechanism of proteins.

Unfolding simulations of Protein L in urea have been investigated extensively (16). However, this is the first time that a comparison of the unfolding trajectories of a protein under different denaturant agents has been carried out in detail. Although the simulations done to investigate the native basin have been performed at 300 K, the unfolding

simulations have been performed at temperatures higher than room temperature, to speed up the physical processes that determine the unfolding of the protein. Because this kind of simulation is very time consuming, performing high-temperature simulations is a common approach (17,18). The simulations in denaturant are compared with simulations performed in pure water to discriminate the net effect of the denaturant, under the approximation that the effects of temperature in the simulations in water alone and in denaturant are similar.

MATERIALS AND METHODS

The simulations were performed in explicit solvent making use of the Gromacs molecular dynamics (MD) package (19) with the Gromos96 force field (G45a1) (20). Water is described with the SPC model. As a rule, the electrostatic interaction implemented with PME, the thermal bath is coupled with the Berendsen algorithm, and the time step is set to 2 fs. Exception is made for the simulations made to study the box of guanidine chloride, which requires a more precise control of the temperature, and thus, in this case, we made use of a Nose-Hoover thermostat. The box is a dodecahedron with a volume of ~100 nm^3.

The parameters of the force field concerning the urea are taken from Smith et al. (21). A 27-nm^3 box of urea is prepared starting from a larger box of 216 nm^3 with 160 urea molecules and 480 water molecules and minimizing the energy while applying an isotropic pressure of 100 bar. For details, see Guerini Rocco et al. (16).

The parameters concerning the interaction of Gdm$^+$, except partial charges, were taken equal to those of arginine in the Gromos96 force field. Partial charges are obtained from density functional theory calculations with a plane-wave basis set and local density approximation (22). Specifically, we first optimized the ionic positions of the isolated molecule. The final partial charges are listed in the second column of Table 1. Making use of such parameters, we carried out 10-ns MD simulations of a 3 M solution of GdmCl. From the simulation we obtained the average electric field acting on a Gdm$^+$ molecule, and the quantum-mechanical optimization was repeated in presence of the electric field. The resulting partial charges are listed in the third column of Table 1. When the procedure was repeated once again, the partial charges changed <5%. These values will thus be used in the following calculations. Note that the charges obtained for the isolated molecule are similar to those used by Mason et al. (23), and the calculations with the electric field provide a more polarized guanidinium molecule.

RESULTS

The guanidine solution

Although the force field that describes urea has been widely tested (16,21), that associated with guanidine is complicated by the large amount of charge involved and consequently is worthy of further investigation.

TABLE 1 Partial charges of Gdm$^+$ atoms from density functional calculations

Atom	Charge (isolated)	Charge (solution)
C	0.692	1.027
N	−0.621	−0.845
H	0.362	0.418

First, it is necessary to show that the force field correctly describes the guanidine molecule in solution. For this purpose, a 10-ns simulation of a 3 M solution of GdmCl in water was performed at 300 K. The resulting radial distribution function (RDF) associated with the N-atoms is displayed in Fig. 1 together with that obtained from neutron diffraction experiments (24). The two main peaks correspond to intramolecular N-N and N-H interactions (peaks corresponding to bonded interaction have been excluded from the plot), whereas the bumps at higher distances are given by correlations between different molecules. The plot shows an overall agreement with the experimental data.

The average density of the simulated solution is 1.041 kg/m^3, compared with the experimental value of 1.049 kg/m^3 (25).

A major problem in the simulation of a GdmCl solution is the long time needed for equilibration starting from a random-generated conformation because of the strong electrostatic interactions present in the solution. To estimate the equilibration time, we make use of the parameter

$$h(t) = \frac{\langle E^2 \rangle_t - \langle E \rangle_t^2}{kT^2 (C_p)_t},$$

where E is the energy of the system, the angular brackets indicate the average calculated over a time interval of duration t from the beginning of the simulation, T is the temperature, and k is the Boltzmann constant. The specific heat $(C_p)_t$ is determined through the finite difference between the average energy calculated in two simulations of duration t performed at temperature T and $T + 10$ K, respectively. The fluctuation-dissipation theorem asserts that h converges to unity at equilibrium. The equality $h = 1$ is a necessary but not sufficient condition for equilibrium; consequently, h can be used, strictly speaking, only to monitor for how long the system is out of equilibrium. The behavior of h as a function of time is displayed in Fig. 2 for two different temperatures and two different concentrations of GdmCl. The 3 M solution
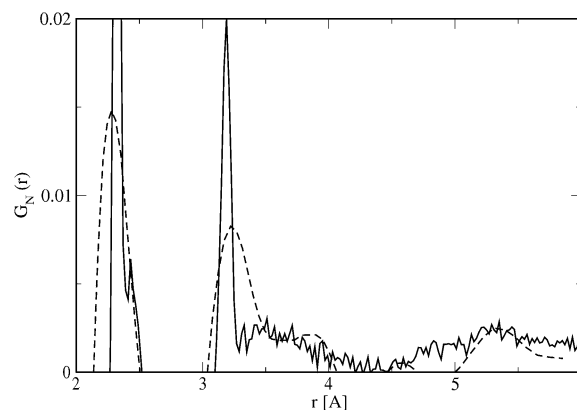

FIGURE 1   RDF of the nitrogens of guanidinium with respect to all other atoms, obtained by MD experiments (*solid curve*) and by neutron diffraction experiments (*dashed curve*, see Mason et al. (24)).
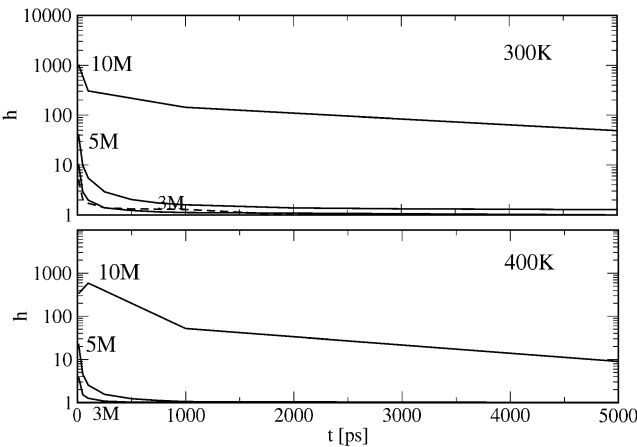
FIGURE 2 Equilibration times for 3 M, 5 M, and 10 M GdmCl solutions and for pure water (*dashed curve*) at 300 K (*top panel*) and 400 K (*bottom panel*).

seems to reach equilibrium (cf. the above caveat) within a few hundreds of picoseconds at both 300 K and 400 K, as in the case of a pure water solution. The 5 M solution equilibrates within the same timescale at 400 K, but at 300 K, it comes close to equilibrium in hundreds of picoseconds but needs nanoseconds to equilibrate completely. The 10 M simulations remain out of equilibrium at both temperatures on the nanosecond time scale. Consequently, the possibility of efficiently simulating 10 M GdmCl solutions was ruled out, and we employed 5 M solutions.

Unfolding of Protein L

The unfolding of Protein L was simulated starting from the crystallographic structure (26) in 5 M GdmCl and in 10 M urea solutions. The results in urea have been extensively discussed (16). A summary of the simulations is listed in Table 2.

TABLE 2 Summary of the simulations

	Solvent	T	Duration
1	Water	400 K	30 ns
2	10 M urea	400 K	30 ns
3	10 M urea	400 K	30 ns
4	5 M GdmCl	400 K	30 ns
5	5 M GdmCl	400 K	20 ns
6	5 M GdmCl	400 K	10 ns
7	Water	480 K	10 ns
8	10 M urea	480 K	10 ns
9	10 M urea	480 K	2 ns
10	5 M GdmCl	480 K	20 ns
11	5 M GdmCl	480 K	7 ns
12	5 M GdmCl	480 K	40 ns
13	10 M urea	300 K	20 ns
14	5 M GdmCl	300 K	20 ns
15	5 M GdmCl*	400 K	20 ns

*This simulation was performed with the force field discussed by Mason et al. (23).

The first set of simulations was performed at 400 K. At this temperature, the protein in water has been observed to unfold in 24 ns in an MD simulation (see Fig. S1 in the Supplementary Material, Data S1). Figs. 3 and 4 display, respectively, the root mean-square deviation (RMSD) and the amount of secondary structure for two simulations performed in urea and GdmCl, respectively. One more simulation in GdmCl is reported in the Supplementary Material (cf. Fig. S2, Data S1) and showed the same qualitative behavior as Fig. 4. In all cases, the breakout of some elements of secondary structures corresponds to a RMSD value of ~0.5 nm. This value is consistent with results obtained with a simplified model (27), according to which the transition state ensemble displays a RMSD of ~0.4 nm and the denatured state of ~0.6 nm. This unfolding event takes place in 16 ns and 17.5 ns in the simulations in urea and in 27 ns, 13 ns, and 4.5 ns in GdmCl. The time at which the RMSD reaches a value of 0.5 nm is then used to compare the structures of the protein with equal degree of unfolding among different simulations.

An important observation is that, in the three unfolding simulations in GdmCl, the α-helix is destabilized fast, whereas the β-sheet is remarkably stable (when the RMSD reaches 0.5 nm, the fractions of residues in α-helix are 0.26, 0.30, and 0, respectively, and those of β-sheet are 0.83, 0.60, and 0.66, respectively). Eventually, the amount of α-helix drops to zero, whereas that of β-sheet remains larger than 0.5. A small loss of β-structure takes place in the residues flanking the helix (see Fig. 5, and Figs. S2 and S3 in the Supplementary Material, Data S1), suggesting that it is related to the elongation of the helical region. The hydrogen bonds between the N- and the C-terminal strands are never observed to
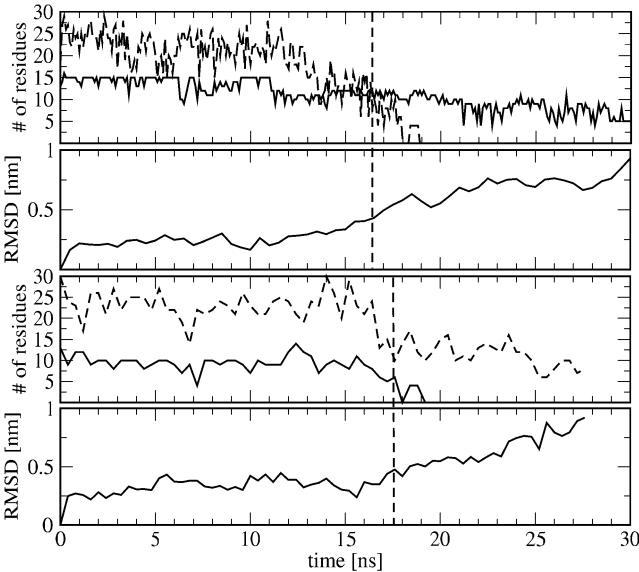

FIGURE 3 Unfolding of Protein L in urea at 400 K in two independent simulations. The first and third panels display the numbers of residues in α-helix (*solid curve*) and β-sheet (*dashed curve*). The second and fourth panels display the associated RMSDs. The vertical dashed line indicates the time at which the RMSD reaches 0.5 nm.
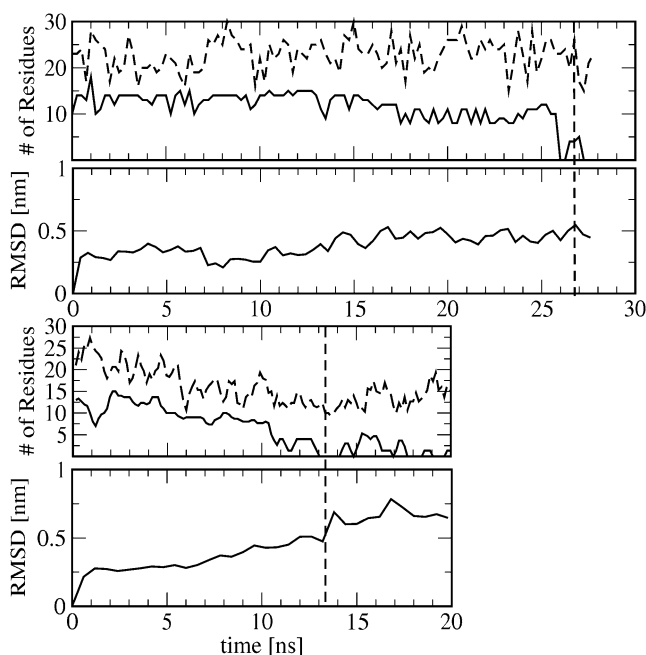
FIGURE 4 Unfolding of Protein L in GdmCl at 400 K in two independent simulations. The first and third panels display the number of residues in α-helix (*solid curve*) and β-sheet (*dashed curve*) in two unfolding simulations. The second and fourth panels are the associated RMSDs. The vertical dashed line indicates the time at which the RMSD reaches 0.5 nm.

break in the simulation time, resulting in transient unfolded conformations as compact as the native one (with a gyration radius of ∼1.2 nm; cf. Fig. S5 in the Supplementary Material, Data S1).

In contrast, in the simulations in urea, unfolding takes place after a considerable destabilization of the β-sheet. In the first simulation, when the RMSD reaches 0.5 nm, the β-sheet is 25% formed (whereas the helix is 80% formed), and eventually the β-sheet is completely unstructured (although the fraction of helical residues remains larger than 30%). The contacts between the N- and C-terminal strands are now lost, although the transient unfolded conformations remain quite compact (the gyration radius being lower than 1.3 nm, see Fig. S6). In the second simulation, when the RMSD overcomes 0.5 nm, the β-sheet is 35% formed (and the helix is 33% formed). Eventually, the fraction of β-sheet drops to 23% and that of α-helix to zero. Interestingly, four to six residues of the native helix assume a β-conformation (cf. Fig. S4 in the Supplementary Material, Data S1).

A further set of simulations has been performed at 480 K in urea and GdmCl. Although at this temperature the protein can also unfold in absence of denaturant within a few nanoseconds (see Fig. S7 in the Supplementary Material, Data S1), it is still interesting to analyze these simulations because all physical processes are faster. The unfolding of Protein L in urea and GdmCl is displayed in Figs. 6 and 7 (cf. also Figs. S8–S12 in the Supplementary Material, Data S1), respectively. In the simulations in urea, both the α-helix and the β-sheet are completely disrupted within a few nanoseconds, and subsequently, the protein elongates, reaching a gyration radius oscillating from 1.5 to 2 nm (cf. Fig. S6, Data S1). The simulations in GdmCl and in pure water, on the other hand, behave similarly to each other: the α-helix is lost in the first 5 ns, whereas the β-sheet is never disrupted completely within the simulation time. Consequently, the radius of gy-
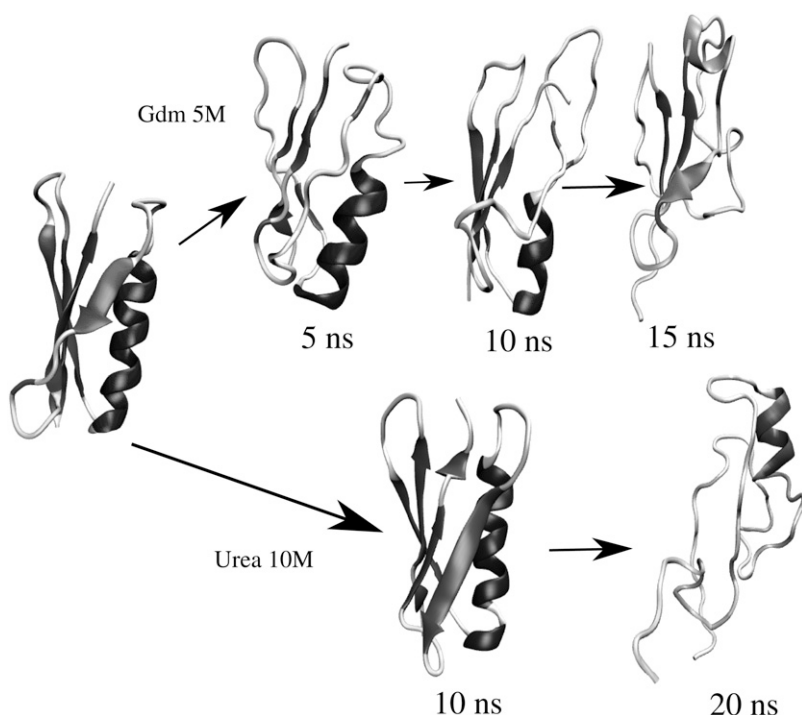

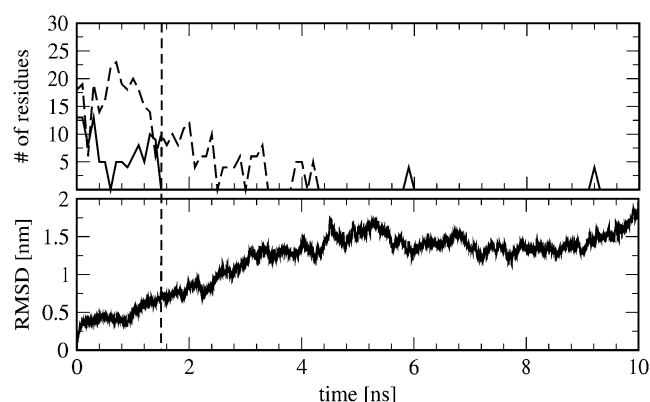FIGURE 5 Snapshots of the unfolding of Protein L at 400K in GdmCl and in urea.

FIGURE 6 Unfolding of Protein L in urea at 480 K (see Fig. 3 legend for details).

ration remains similar to that of the folded protein (i.e., <1.3 nm; cf. Fig. S5, Data S1). These results are compatible with the picture described above and, furthermore, indicate that the β-sheet is long-lived unless one adds urea to the solution.

Structure of the solution around the native state of Protein L

To understand the different mechanisms that trigger denaturation of Protein L in urea and GdmCl, we performed a set of 20-ns simulations at 300 K, at which temperature the protein is not able to escape from its native basin (the RMSD is lower than 3 Å) and consequently can provide structural information about the native metastable state.

Fig. 8 displays the correlation between the total RMSD of the protein and the RMSD of the α- and β-structures in urea and GdmCl, respectively. The simulation in urea shows a strong correlation (correlation coefficient $r = 0.984$) between the degree of formation of the whole protein and of its β-structure, and no correlation ($r = -0.172$) with the degree of formation of the α-helix, supporting the idea that unfolding starts in the native state by denaturation of the β-sheet.

The RDF of urea and water with respect to the protein, calculated in the 20-ns simulation in urea, is displayed in Fig. 9 (*left panel*) together with the RDF of water in a 20-ns
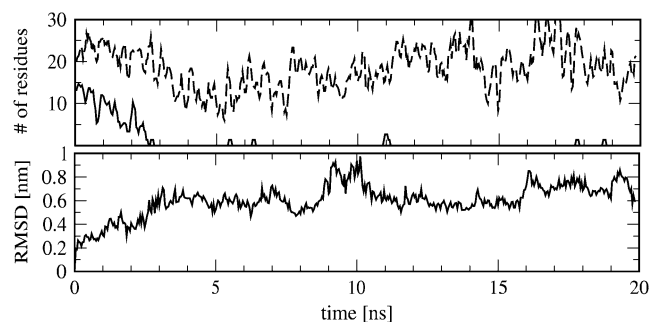

FIGURE 7 Unfolding of Protein L in GdmCl at 480 K (see Fig. 4 legend for details).

simulation of the protein in pure water. The RDF in all cases displays a peak at 0.17 nm, corresponding to the atoms belonging to the first shell of solvent molecules closest to the protein. With respect to the simulation in pure water, one can observe that in the simulation in urea the density of water molecules in the first shell drops and is compensated by molecules of urea. Integrating the RDF over the first shell of solvent (i.e., up to 0.35 nm, which is the typical donor-acceptor distance in hydrogen bonds), one deduces that in pure water this is composed of 154.9 water molecules, whereas in urea solution it is composed of 65.3 urea molecules and 37.2 water molecules. Note that the ratio $65.3{:}37.2 = 1.8$ is much higher than the ratio $816{:}3384 = 0.24$ between the total number of urea and water molecules in the system. This wide difference suggests that the increase in urea density around the protein is caused by an attractive mechanism (which can be a direct interaction or an effective, entropy-mediated interaction). This effect cannot be explained in terms of the number of hydrogen bonds between the protein and the solvent: in pure water the mean number of such bonds is 140.1, a number that decreases to 49.8 on addition of urea (44.6 between protein and urea, 5.2 between protein and water).

The effect of GdmCl on the secondary structures of Protein L is symmetrical to that of urea in the sense that the total RMSD is more correlated to that of the α-helix ($r = 0.73$) than to that of the β-sheet ($r = 0.50$, cf. Fig. 8). The largest (former) correlation is smaller than in the case of urea, most likely because the overall structural fluctuations are smaller in GdmCl (i.e., the total RMSD ranges between 0.18 and 0.28 nm in GdmCl and between 0.11 and 0.31 nm in urea). More interestingly, in GdmCl there are detectable correlations with both α- and β-structures, indicating that the interaction is less specific with respect to the kind of secondary structure.

The structure of the GdmCl solution around the protein, described by the RDF shown in the right panel of Fig. 9, is markedly different from that of the urea solution. The structure of water is essentially identical to that observed in pure water. Also, the distribution of GdmCl is similar to that of water, especially in the first shell around the protein. This implies that the density of water and GdmCl molecules in the first shell is essentially the same as in the bulk solution. The mean number of hydrogen bonds between GdmCl and the protein is 28.7, whereas that between water and the protein is 75.2. As in the case of the urea solution, the total number of hydrogen bonds between the solvent and the protein is lower than in the case of pure water, but in this case GdmCl can build fewer bonds than water.

The average dipole moment generated by the GdmCl solution is 136.3 D, a number that should be compared with that generated by the pure-water solution (15.1 D). This indicates that the protein induces a polarization of Gm^+ and Cl^- that, in turn, applies an electric field to the protein. Fig. 10 displays the potential (calculated after Baker et al. (28)) that the solvent causes on the surface of the protein. One can observe that, unlike pure water, the GdmCl solution causes a dif-
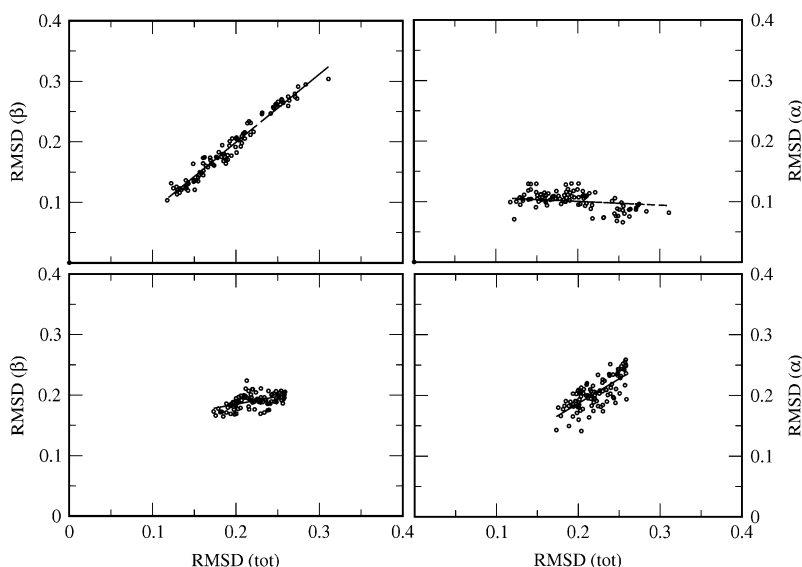
FIGURE 8 Correlation between the total RMSD of the protein and the RMSD of α- and β-structures in the 300 K simulation around the native conformation in urea (*upper panels*) and GdmCl (*lower panels*). The dashed line indicates the linear regression, which gives correlation coefficients $r = 0.984$ for β-structure and $r = -0.172$ for α-structure in urea, and $r = 0.50$ for β-structure and $r = 0.73$ for α-structure in GdmCl.

ference of potential between the two ends of the helix of several kT/e.

DISCUSSION

The main result of the work presented here is that the unfolding pathway of Protein L in GdmCl is different from that in urea and involves first the destabilization of the α-helix in the former case and of the β-sheet in the latter. The structural characterization of the free energy minimum corresponding to the denatured state is still computationally out of question. Our simulations account only for the initial stages of un-

folding, as they describe few tens of nanoseconds, to be compared with the overall unfolding time of 300 ms of Protein L in 5 M GdmCl (13). Nonetheless, the differing effect of GdmCl and urea on the different secondary structures of the protein allows one to speculate that the two unfolded states can be structurally (but not thermodynamically (5,6)) different.

Within this context, the simulations carried out at 480 K are of particular interest because such a high temperature speeds up all physical processes. These show that GdmCl is not able to break the β-sheet in the whole simulation time, even if the helix gets unstructured in the first few nanoseconds. On the other hand, the simulations in urea show that, after the β-sheet is disrupted, the helix is also lost in a few nanoseconds. These data suggest that the intrinsic role of the β-sheet and of the α-helix are asymmetric, the former being more critical for the overall stability of the protein.

The disruption of the helix and the robustness of the β-structure observed in the simulations in GdmCl are compatible with NMR experiments of Protein L performed in 3 M GdmCl (29). In fact, the chemical shifts, the medium-range
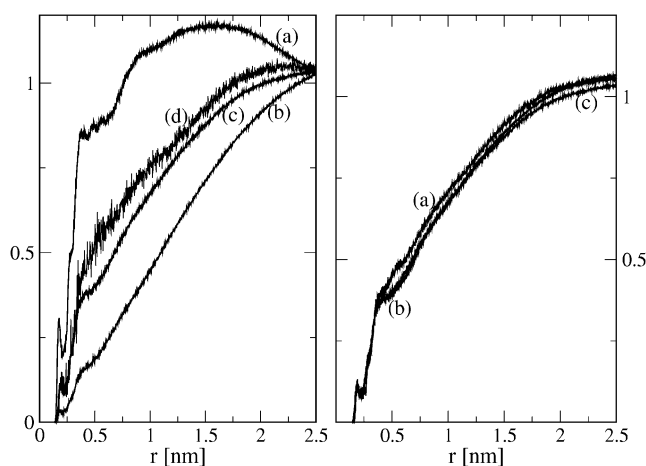

FIGURE 9 RDF calculated in the 300 K simulation in urea (*left panel*) and GdmCl (*right panel*). The total RDF, calculated between all the atoms of the denaturant and all the atoms of the protein (*a*), the total RDF between all the water atoms and all the atoms of the protein (*b*), and, as reference, the total RDF between all the water atoms and all the protein atoms in a simulation in pure water (*c*). In the case of GdmCl, the total RDF of denaturant with respect to the protein, calculated at 3 M GdmCl is also displayed (*d*).
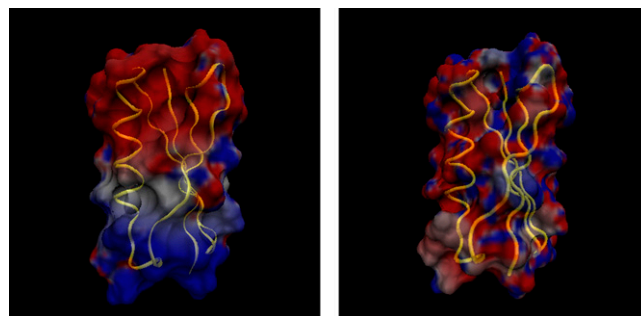

FIGURE 10 Electrostatic potential generated by the solution on the surface of Protein L in 5 M GdmCl (*left*) and in water (*right*) at 300 K. The colors range from red ($V = -10 \ kT/e$) to blue ($V = +10 \ kT/e$).

nuclear Overhauser effect signals, and the oscillations in the profile of paramagnetic-relaxation-enhancement experiments indicate the presence of consistent residual structure in the first hairpin but not in the helix. Moreover, the results of the simulations are also compatible with the results of ϕ-value analysis, which indicate that the first hairpin, but not the helix, is structured in the transition state between the native and the GdmCl-stabilized denatured state (13–15). Similar experiments in urea, which are not available in the literature, would be welcome to validate our computational findings.

As compared with urea, building a computational model for GdmCl displays two further problems. First, molecular polarizability seems to play an important role, as a consequence of the strong local electric field created by the large quantity of ions in solution. The zero-order solution, employed here, is to account for the electric field in the quantum calculation performed to obtain the partial charges and use these (fixed) values for the classical simulations.

Simulations of aqueous solution of GdmCl have been performed in the past (23) to characterize the structural properties of the solution. In that work, the partial charges were that of arginine in CHARMM22, which is 0.64 for C, -0.80 for N, and 0.46 for H. In a 20-ns simulation at 400 K in 5 M GdmCl using these partial charges, the RMSD does not increase above 0.4 nm, and the secondary structure remains intact (cf. Fig. S13, Data S1). The comparison of these results with ours seems to indicate that the careful calculation of the partial charges (as described in Materials and Methods) is critical to describe correctly the unfolding ability of GdmCl on proteins.

Recent calculations have been performed using the same force field as that of Mason et al. (23), simulating the dynamics of methane, of the H1 helix of mouse prion (30), and of the melittin helical peptide (31). The main difference between these and our calculations is that we do not observe a net increase of Gdm^+ in the first shell of solvent around the protein but a polarization of Gdm^+ and Cl^-. There can be several reasons for this difference. First, we simulate a 5 M GdmCl solution, whereas O'Brien et al. (30) and Mason et al. (31) used a 3 M solution. In fact, repeating the simulation at 3 M concentration produces an RDF more similar to that displayed in Fig. 7 of O'Brien et al. (30) (cf. the curve d in the *left panel* of Fig. 9). This result highlights a concentration effect that was already noted in the case of methane (cf. Fig. 5 of O'Brien et al. (30)). Moreover, the systems studied by O'Brien et al. (30) and Mason et al. (31) are considerably smaller than Protein L, something that can again affect the equilibrium distribution of charges.

The other difficulty associated with simulations of a GdmCl solution is that at high concentration the dynamics of molecules becomes slower, and consequently, simulations of a few nanoseconds become meaningless. This phenomenon is likely to be associated with the strong network of Coulomb interactions produced by the large quantity of charges in the solution. As a matter of fact, the viscosity of GdmCl solutions

is known (32) to be highly nonlinear with concentrations above 4 M. The concentration of 5 M GdmCl used above is a tradeoff between denaturing power and ability to diffuse, a quantity to which the unfolding rate is related.

The different unfolding pathways in urea and GdmCl are reflected by the different structures of the solvent around the protein. Urea accumulates in the first shell, pulling away water and lowering the total number of hydrogen bonds between the protein and the solvent. This perturbation of the structure of water extends to the whole volume. Consequently, protein unfolding takes place both because of the direct interaction between urea and the protein and because of the variation of the structure of the solvent (and thus of the hydrophobic effect). GdmCl, on the other hand, does not appreciably change the static properties of the solution. The average dipole moment generated by the GdmCl solution is much larger than that generated by water. This allows for the speculation that unfolding is associated with the Coulomb interaction between GdmCl and the protein. In particular, the helical region of Protein L is rich in residues that, at neutral pH, are charged (7 of 17, i.e., 25E, 26K, 30E, 36D, 39K, 40K, and 41D). Within the dipolar electric field generated by the Gdm^+ and Cl^- ions, the charged residues stretch the α-helix, causing its unfolding. On the other hand, the fraction of charged residues in the β-sheet is lower (9 of 43). Because the Coulomb interactions are long-ranged, this can be done without perturbing the first shell of solvent.

CONCLUSIONS

A detailed comparison of the unfolding trajectories of a model protein in solution with urea and GdmCl has been carried out for the first time. The unfolding of Protein L follows two different pathways in urea and in GdmCl. This suggests that the effects of the specific kind of denaturant should be accounted for in interpreting folding and unfolding experiments, especially when the protein is monitored through the degree of formation of its secondary structure. To perform the simulations that provided these results, we developed a force field to describe guanidinium. This force field improves the parametrization described by Mason et al. (23), taking into account, in a very simple way, some polarization effects.

SUPPLEMENTARY MATERIAL

To view all of the supplemental files associated with this article, visit www.biophysj.org.

REFERENCES

1. Tanford, C., K. Kawahara, and S. Lapanje. 1966. Proteins in 6 M guanidine hydrochloride. Demonstration of random coil behaviour. *J. Biol. Chem.* 241:1921–1923.

2. Greene, R. F., and C. N. Pace. 1974. Urea and guanidine hydrochloride denaturation of ribonuclease, lysozyme, α-chymotrypsin, and β-lactoglobulin. *J. Biol. Chem.* 249:5388–5394.

3. Fersht, A. 1999. Structure and Mechanism in Protein Science. W. H. Freeman, New York.

4. Shortle, D. 1996. The denatured state (the other half of the folding equation) and its role in protein stability. *FASEB J.* 10:27–34.

5. Pfeil, W., and P. L. Privalov. 1976. Thermodynamic investigations of proteins. II. Calorimetric study of lysozyme denaturation by guanidine hydrochloride. *Biophys. Chem.* 4:33–40.

6. Makhatadze, G. I., and P. L. Privalov. 1992. Protein interactions with urea and guanidinium chloride. A calorimetric study. *J. Mol. Biol.* 226:491–505.

7. Shellman, J. A. 1955. The thermodynamics of urea solutions and the heat of formation of the peptide hydrogen bond. *C. R. Trav. Lab. Carlsberg.* 29:223–229.

8. Kresheck, G. C., and H. A. Scheraga. 1965. The temperature dependence of the enthalpy of formation of the amide hydrogen bond; the urea model. *J. Phys. Chem.* 69:1704–1706.

9. Frank, H. S., and F. Franks. 1968. Structural approach to the solvent power of water for hydrocarbons; urea as a structure breaker. *J. Chem. Phys.* 48:4746–4757.

10. Santoro, M. M., and D. W. Bolen. 1988. Unfolding free energy changes determined by the linear extrapolation method. 1. Unfolding of phenylmethanesulfonyl α-chymotrypsin using different denaturants. *Biochemistry.* 27:8063–8068.

11. Rezus, Y. L. A., and H. J. Bakker. 2006. Effect of urea on the structural dynamics of water. *Proc. Natl. Acad. Sci. USA.* 103:18417–18420.

12. Möglich, A., F. Krieger, and T. Kiefhaber. 2005. Molecular basis for the effect of urea and guanidinium chloride on the dynamics of unfolded polypeptide chains. *J. Mol. Biol.* 345:153–162.

13. Scalley, M. L., Q. Yi, H. Gu, A. McCormack, J. R. Yates, and D. Baker. 1997. Kinetics of folding of the IgG binding domain of peptostreptococcal protein L. *Biochemistry.* 36:3373–3382.

14. Scalley, M. L., S. Nauli, S. T. Gladwin, and D. Baker. 1999. Structural transitions in the protein L denatured state ensemble. *Biochemistry.* 38:15927–15935.

15. Kim, D. E., Q. Yi, S. T. Gladwin, J. M. Goldberg, and D. Baker. 1998. The single helix in protein L is largely disrupted at the rate-limiting step in folding. *J. Mol. Biol.* 284:807–815.

16. Guerini Rocco, A., L. Mollica, P. Ricchiuto, A. Baptista, E. Gianazza, and I. Eberini. 2008. Characterization of the protein unfolding processes by urea and temperature. *Biophys. J.* 94:2241–2251.

17. Bennion, B. J., and V. Daggett. 2003. The molecular basis for the chemical denaturation of proteins by urea. *Proc. Natl. Acad. Sci. USA.* 100:5142–5147.

18. Wang, T., and R. C. Wade. 2007. On the use of elevated temperature in simulations to study protein unfolding mechanisms. *J. Chem. Theory Comput.* 3:1476–1483.

19. Berendsen, H. J. C., D. van der Spoeland, and R. van Drunen. 1995. GROMACS: a message-passing parallel molecular dynamics implementation. *Comput. Phys. Commun.* 91:43–56.

20. Schuler, L. D., X. Daura, and W. F. van Gunsteren. 2001. An improved GROMOS 96 force field for aliphatic hydrocarbons in the condensed phase. *J. Comput. Chem.* 22:1205–1218.

21. Smith, L. J., R. M. Jones, and W. F. van Gunsteren. 2005. Characterization of the denaturation of human-lactalbumin in urea by molecular dynamics simulations. *Proteins.* 58:439–449.

22. Car, R., and M. Parrinello. 1985. Unified approach for molecular dynamics and density-functional theory. *Phys. Rev. Lett.* 55:2471–2474.

23. Mason, P. E., G. W. Neilson, J. E. Enderby, M. L. Saboungi, C. E. Dempsey, D. MacKerell, and J. W. Brady. 2004. The structure of aqueous guanidinium chloride solutions. *J. Am. Chem. Soc.* 126:11462–11470.

24. Mason, P. E., G. W. Neilson, C. E. Dempsey, A. C. Barnes, and J. M. Cruickshank. 2003. The hydration structure of guanidinium and thiocyanate ions: Implications for protein stability in aqueous solution. *Proc. Natl. Acad. Sci. USA.* 100:4557–4561.

25. Kawahara, K., and C. Tanford. 1966. Viscosity and density of aqueous solutions of urea and guanidine hydrochloride. *J. Biol. Chem.* 241:3228–3232.

26. Wikstroem, M., U. Sjoebring, W. Kastern, L. Bjoerck, T. Drakenberg, and S. Forsen. 1993. Proton nuclear magnetic resonance sequential assignments and secondary structure of an immunoglobulin light chain-binding domain of protein L. *Biochemistry.* 32:3381–3386.

27. Amatori, A., G. Tiana, J. Ferkinghoff-Borg, and R. A. Broglia. 2008. The denatured state is critical in determining the properties of model proteins designed on different folds. *Proteins.* 70:1047–1055.

28. Baker, N. A., D. Sept, S. Joseph, M. J. Holst, and J. A. McCammon. 2001. Electrostatics of nanosystems: application to microtubules and the ribosome. *Proc. Natl. Acad. Sci. USA.* 98:10037–10041.

29. Yi, Q., L. Scalley-Kim, E. J. Alm, and D. Baker. 2000. NMR characterization of residual structure in the denatured state of protein L. *J. Mol. Biol.* 299:1341–1351.

30. O'Brien, E. P., R. I. Dima, B. Brooks, and D. Thirumalai. 2007. Interactions between hydrophobic and ionic solutes in aqueous guanidinium chloride and urea solutions: lessons for protein denaturation mechanism. *J. Am. Chem. Soc.* 129:7346–7353.

31. Mason, P. E., J. W. Brady, G. W. Neilson, and C. E. Dempsey. 2007. The interaction of guanidinium ions with a model peptide. *Biophys. J.* 93:L04–L07.

32. Perl, D., M. Jacob, M. Bano, M. Stupak, M. Antalikand, and F. X. Schmid. 2002. Thermodynamics of a diffusional protein folding reaction. *Biophys. Chem.* 96:173–190.